

Metal-Drug Interactions: Synthesis and Spectroscopic Characteristics, Surface Morphology, and Pharmacological Activity of Ephedrine–HCl Complexes with Mo(V), Nb(V), Ga(III), and Ge(IV)

A. A. El-Habeeb^a and M. S. Refat^{b,c*}

^a College of Science, Princess Nourah Bint Abdulrahman University, Department of Chemistry, Riyadh, Saudi Arabia

^b Chemistry Department, Faculty of Science, Taif University, P.O. Box 888, Al-Hawiah, Taif, 21974 Saudi Arabia

^c Department of Chemistry, Faculty of Science, Port Said University, Port Said, Egypt

*e-mail: msrefat@yahoo.com

Received July 2, 2018

Abstract—Four new Mo(V), Nb(V), Ga(III), and Ge(IV) ephedrine complexes, $[\text{Mo}(\text{Eph})_2(\text{Cl})_4]\text{Cl}$, $[\text{Nb}(\text{Eph})_2(\text{Cl})_3]$, $[\text{Ga}(\text{Eph})_2(\text{Cl})_3]$, and $[\text{Ge}(\text{Eph})_2(\text{Cl})_2]$ are synthesized and characterized. Composition and coordination behavior of ephedrine drug towards Mo(V), Nb(V), Ga(III), and Ge(IV) ions are deduced from microanalysis, IR spectra, molar conductance, magnetic and thermal analysis data. These support coordination of the eph ligand in its neutral state. Ephedrine has two powerful chelating sites, OH and NH, that determine its uni- or bidentate mode of action. IR spectra indicate that Mo(V) and Ga(III) coordinate to ephedrine via nitrogen atom of the NH group as a unidentate chelator with six and five coordination geometry, respectively. On the other hand, Eph ligand behaves as a monoanionic bidentate no chelating agent via the NH and deprotonated OH groups in Nb(V) and Ge(IV) complexes. Mo(V) complex demonstrates electrolytic properties, the other complexes are non-electrolytes in DMSO solutions. TG/DTG analysis makes it possible to calculate the number of solvent molecules in and outside the coordination sphere, and estimate stability of the synthesized complexes. The Eph complexes are screened *in vitro* for antibacterial (*Escherichia coli*, *Pseudomonas aeruginosa*, *Bacillus subtilis* and *Staphylococcus aureus*) and antifungal (*Aspergillus flavus* and *Candida albicans*) activities. Anti-cancer action of the Mo(V) and Ga(III) complexes is assessed against the human hepato cellular carcinoma (HepG-2) tumor cell line ($\text{IC}_{50} > 1000 \mu\text{g/mL}$).

Keywords: Ephedrine, Mo(V), Nb(V), Ga(III), Ge(IV), spectroscopic, chelation, anticancer activity

DOI: 10.1134/S1070363218100225

INTRODUCTION

According to pharmacological studies ephedrine is a sympathomimetic agonist at both α - and β -adrenergic receptors, with specific modes of action [1, 2] that include also some side effects [3]. Biological properties of complexes are dependent predominantly on the oxidation state of a metal, the coordination number and kind of a coordinated ligand, and their structural features [4–9]. In the current study, we evaluated the probability of ephedrine interaction with the title metal ions.

EXPERIMENTAL

Analytical grade ephedrine hydrochloride drug (Fig. 1), MoCl_5 , NbCl_5 , GaCl_3 , and GeCl_4 salts were

purchased from Sigma-Aldrich Chemical Corporation, St. Louis, Mo, USA, and used without further purification.

Elemental analyses was carried out on a Perkin Elmer CHN 2400 (USA). Molar conductivities of freshly prepared $1.0 \times 10^{-3} \text{ mol/cm}^3$ DMSO solutions were measured on a Jenway 4010 conductivity meter. IR spectra were recorded on a Bruker FTIR Spectrophotometer ($4000\text{--}400 \text{ cm}^{-1}$). UV-Vis absorption spectra were recorded in DMSO within $800\text{--}200 \text{ nm}$

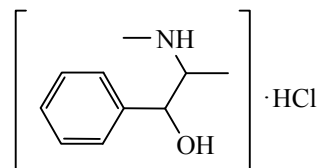


Fig. 1. Formula of Ephedrine hydrochloride drug (Eph).

¹ The text was submitted by the authors in English.

range on a UV2 Unicam UV/Vis Spectrophotometer fitted with a quartz cell of 1.0 cm path length. Magnetic moments were calculated using the Magnetic Susceptibility Balance, Sherwood Scientific, Cambridge Science Park, Cambridge, England, at 25°C. The thermal studies TG/DTG–50H were carried out on a Shimadzu thermo-gravimetric analyzer under the atmosphere of nitrogen up to 800°C. Scanning electron microscopy (SEM) images were taken on a Quanta FEG 250 equipment. X-Ray diffraction patterns were measured on a X'Pert PRO PANalytical X-ray powder diffractometer. Transmission electron microscopy images (TEM) were taken on a JEOL 100s microscope.

[Mo(Eph)₂(Cl)₄]·Cl (1). A mixture of 1.0 mmol of MoCl₅ with 2.0 mmol of ephedrine HCl in methanol (25 mL) was neutralized to pH = 8–9 using NH₄OH, then refluxed for 3 h, giving a brown solution which was concentrated and stored for one week yielding a brown precipitate, yield 61%. $T_{dec} = 225^{\circ}\text{C}$. Found, %: C 39.65; H 4.97; N 4.61; Cl 29.12. Calculated, %: C 39.79; H 5.01; N 4.64; Cl 29.36. $\Lambda_M = 66 \Omega^{-1} \text{cm}^2 \text{mol}^{-1}$.

The complexes 2–4 were synthesized as above.

[Nb(Eph)₂(Cl)₃] (2). Yield 69%. $T_{dec} = 260^{\circ}\text{C}$. Found, %: C 45.33; H; 5.23; N 5.12; Cl 20.09. Calculated, %: C 45.52; H 5.23; N 5.31; Cl 20.15. $\Lambda_M = 14 \Omega^{-1} \text{cm}^2 \text{mol}^{-1}$.

[Ga(Eph)₂(Cl)₃] (3). Yield 66%. $T_{dec} = 266^{\circ}\text{C}$. Found, %: C 47.12; H 5.87; N 5.48; Cl 20.98. Calculated, %: C 47.42; H 5.87; N 5.48; Cl 20.98. $\Lambda_M = 19 \Omega^{-1} \text{cm}^2 \text{mol}^{-1}$.

[Ge(Eph)₂(Cl)₂] (4). Yield 60%. $T_{dec} = 270^{\circ}\text{C}$. Found, %: C 50.76; H 5.87; N 5.78; Cl 14.98. Calculated, %: C 50.89; H 5.98; N 5.94; Cl 15.02. $\Lambda_M = 16 \Omega^{-1} \text{cm}^2 \text{mol}^{-1}$.

Antimicrobial assessments. Antimicrobial activity of the tested samples was determined using the modified Kirby-Bauer disc diffusion method [10]. Briefly, 100 μL of the tested bacteria [*G*⁺ (*Escherichia coli* and *Pseudomonas aeruginosa*), *G*⁻ (*Bacillus subtilis* and *Staphylococcus aureus*), fungi (*Aspergillus flavus* and *Candida albicans*)] were grown in 10 mL of fresh media until they reached a count of approximately 10⁸ cells/mL for bacteria or 10⁵ cells/mL for fungi [11]. 100 μL Of microbial suspension was spread onto agar plates corresponding to the broth in which they were maintained. Isolated colonies of each organism that might be playing a pathogenic role should be selected from primary agar plates and tested

for susceptibility by the disc diffusion method [12, 13].

Anti-cancer activities. The mammalian cell lines: HepG-2 cells (human Hepatocellular carcinoma) were obtained from VACSERA Tissue Culture Unit. Chemicals used: DMSO) crystal violet and trypan blue dyes were purchased from Sigma (St. Louis, Mo., USA). Fetal Bovine serum, DMEM, RPMI-1640, HEPES buffer solution, L-glutamine, gentamycin and 0.25% Trypsin-EDTA were purchased from Lonza.

Crystal violet stain (1%) was composed of 0.5% (w/v) crystal violet and 50% methanol. It was adjusted to the appropriate volume with dd H₂O and filtered through a Whatmann No.1 filter paper. Cell line propagation: The cells were propagated in Dulbecco's modified Eagle's medium (DMEM) supplemented with 10% heat-inactivated fetal bovine serum, 1% L-glutamine, HEPES buffer and 50 $\mu\text{g}/\text{mL}$ gentamycin. All cells were maintained at 37°C in a humidified atmosphere with 5% CO₂ and subcultured two times a week. Cytotoxicity evaluation using the viability assay [14, 15]: for cytotoxicity assay, the cells were seeded in 96-well plate at a cell concentration of 1×10⁴ cells per well in 100 μL of growth medium. Fresh medium containing different concentrations of the test sample was added after 24 h of seeding. Serial two-fold dilutions of the tested chemical compound were added to confluent cell monolayers dispensed into 96-well, flat-bottomed microtiter plates (Falcon, NJ, USA) using a multichannel pipette. The microtiter plates were incubated at 37°C in a humidified incubator with 5% CO₂ for a period of 48 h. Three wells were used for each concentration of the test sample. Control cells were incubated without test sample and with or without DMSO. DMSO present in the wells (max 0.1%) was found not to affect the experiment. After incubation of the cells at 37°C, various concentrations of sample were added, the incubation was continued for 24 h and viable cells yield was determined by a colorimetric method. In brief, after the end of the incubation period, media were aspirated and the crystal violet solution (1%) was added to each well for at least 30 min. The stain was removed and the plates were rinsed using tap water until all excess stain is removed. Glacial acetic acid (30%) was then added to all wells and mixed thoroughly, and then the absorbance of the plates were measured upon gentle shaking on a Microplate reader (TECAN, Inc.), using a test wavelength of 490 nm. All results were corrected for background absorbance detected in wells without

Table 1. Assignments of the FT-IR essential bands (cm^{-1}) of Eph-HCl and its metal complexes **1–4**

Compound	$\nu(\text{OH})$	$\nu(\text{NH})$	δ_{OH} (out-of-plane)	$\nu(\text{C-O})$	δ_{OH} (in-plane)	δ_{NH}	$\nu(\text{M-Cl})$	$\nu(\text{M-N})$	$\nu(\text{M-O})$
Eph-HCl	3331	2976	752	1049	1394	1590	–	–	–
1	3330	2990	752	1049	1398	1598	320	450	–
2	3143	2993	751	1049	–	1590	294	523	450
3	3331	2941	752	1049	1395	1589	338	449	–
4	3147	3042	–	1049	–	–	314	484	451

added stain. Treated samples were compared with the cell control in the absence of the tested compounds. All experiments were carried out in triplicate. The cell cytotoxic effect of each tested compound was calculated. The optical density was measured with the microplate reader (SunRise, TECAN, Inc, USA) to determine the number of viable cells and percentage of viability was calculated as $[1 - (\text{OD}_t/\text{OD}_c)] \times 100\%$, where OD_t is the mean optical density of wells treated with the tested sample, and OD_c is the mean optical density of untreated cells. The relation between surviving cells and drug concentration was plotted to get the survival curve of each tumor cell line after treatment with the specified compound. The 50% inhibitory concentration (IC_{50}), was estimated from graphic plots of the dose response curve for each concentration using Graphpad Prism software (San Diego, CA. USA).

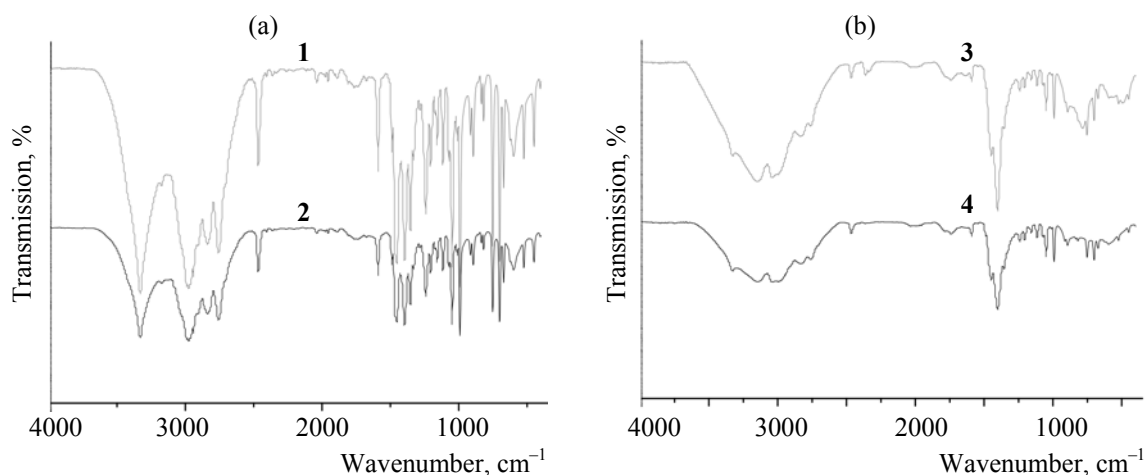
RESULTS AND DISCUSSION

Stoichiometry and molar conductance. All isolated complexes of ephedrine with Mo(V), Nb(V), Ga(III), and Ge(IV) were stable in the air, insoluble in water, soluble in DMF and DMSO, but poorly soluble

in the other common organic solvents. The solutions of complexes of Nb(V), Ga(III) and Ge(IV) (**2–4**) in DMSO demonstrated low conductance ($\Lambda_m = 14\text{--}19 \Omega^{-1} \text{cm}^2 \text{mol}^{-1}$) supporting their non-electrolyte nature unlike the complex $[\text{Mo}(\text{Eph})_2(\text{Cl})_4] \cdot \text{Cl}$, that exhibited the electrolytic nature ($\Lambda_m = 66 \Omega^{-1} \text{cm}^2 \text{mol}^{-1}$) due to the presence of one chlorine anion outside the coordination sphere [16]. TGA experiments indicated the unhydrous structure of the complexes **1–4**.

IR spectra. In the IR spectrum of free ephedrine hydrochloride chelate (Table 1) the significant broadening of the bands assigned to the OH and NH groups was observed. This supported the effect of intraligand H-bonding between the two neighbouring groups. Possibility of such bond was also supported by molecular modelling [17, 18].

The profiles of FT-IR spectra of the Mo(V) and Ga(III) ephedrine complexes and both Nb(V) and Ge(IV) ephedrine complexes **1** and **3** demonstrated similarity, as well as some overlapping was observed for the spectra of complexes **2** and **4** (Figs. 2a, 2b). These clear similarity between the spectra within the certain pairs of complexes reflected two different

**Fig. 2.** FT-IR spectra of the complexes (a) (1) **1**, (2) **2** and (b) (3) **3**, (4) **4**.

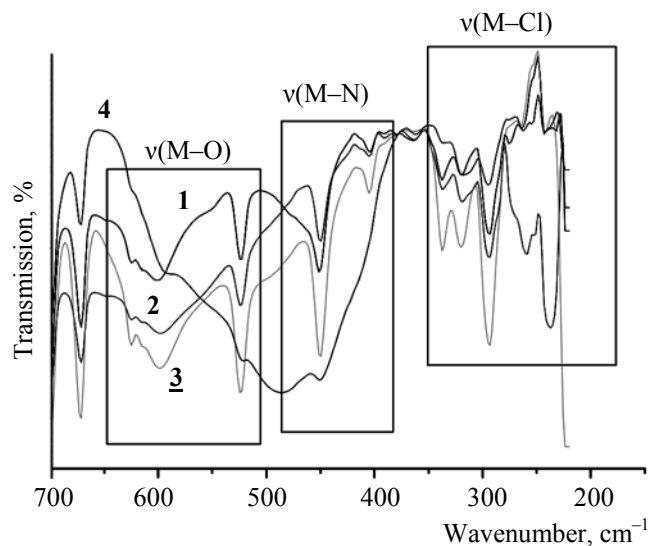


Fig. 3. FT-IR spectra of Eph complexes 1–4.

modes of coordination. In the IR spectra of the complexes 2 and 4 the bands assigned originally to NH at 2975 cm^{-1} and OH at 3331 cm^{-1} groups of free Eph ligand became lower or annihilated that could be attributed to their involvement in chelation [19, 20]. The band of free Eph spectrum at 1098 cm^{-1} assigned to $\delta(\text{CH})$ with the strong contribution of $\nu(\text{C-O})$ [21] demonstrated lower intensity upon complexation. The bands derived from the aromatic ring out-of-plane bending modes recorded at 701 and 672 cm^{-1} in the spectrum of the ligand demonstrated shifts towards lower wave-numbers in the spectra of complexes. Such effect could be caused by the disturbance of the aromatic system by deforming the uniform distribution of π -electron charges in the ring [22]. The spectral region around 1000 cm^{-1} demonstrated similar patterns for the Eph complexes. The most intense band was assigned tentatively to the in-plane bonding $\delta(\text{CH})$ [23]. According to spectral data in Mo(V) and Ga(III) complexes Eph acted as a unidentate chelate via interaction with nitrogen atom of the NH group. The new bands assigned to $\nu(\text{M-N})$ and $\nu(\text{M-O})$ [20] were detected in the low frequency field, unlike $\nu(\text{M-Cl})$ that could be detectable only in the far-IR spectra (Fig. 3, Table 1).

Electronic and magnetic measurements. The UV-Vis spectrum of EphHCl drug (Fig. 4) demonstrated two absorption bands at 275 and 289 nm assigned to $\pi-\pi^*$ and $n-\pi^*$ transitions, respectively. The latter band disappeared or shifted to higher or lower wavelength upon Eph coordination with metals [24]. The broad or shoulder bands at 334 and 382 nm for

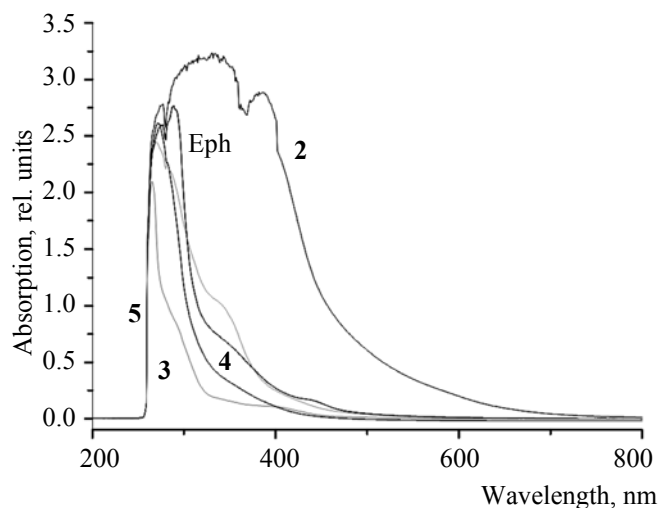


Fig. 4. UV-Vis spectra of free Eph hydrochloride drug and its complexes 1–4.

Mo(V)–Eph complex, 397 nm for Nb(V)–Eph complex, and 341 nm for Ge(IV)–Eph complex were assigned to $L\rightarrow M$ and $M\rightarrow L$ charge transfer transitions (Fig. 4). Absence of absorption bands above 400 nm indicated d^0 -configuration of the complexes. The effective magnetic moments (μ_{eff}) of the complexes 1–4 were measured at room temperature. The monomeric Mo(V) complex six-coordinate octahedral structure was supported by the magnetic moment (1.43 Bohr magneton). Nb(V) complex was diamagnetic as expected for its d^0 state, and its possible structure could be seven coordinate with the NH and OH groups involved in coordination. The experimental magnetic data of Ga(III) and Ge(IV) complexes confirmed their diamagnetic nature with coordination modes being five and six, respectively [25, 26].

So, Eph chelator behaved as a uni- or bidentate ligand via coordination with its NH nitrogen and/or oxygen of the deprotonated OH group towards the central metal atoms (Fig. 5).

Thermogravimetric analyses. TGA–DrTGA curves of anhydrous complexes $[\text{Mo}(\text{Eph})_2(\text{Cl})_4]\cdot\text{Cl}$, $[\text{Nb}(\text{Eph})_2(\text{Cl})_3]$, $[\text{Ga}(\text{Eph})_2(\text{Cl})_3]$, and $[\text{Ge}(\text{Eph})_2(\text{Cl})_2]$ demonstrated their thermal decomposition in one-to-three degradation stages indicated by differential thermogravimetric peaks $\text{DTG}_{\text{max}} = 224, 294$ and 482°C , 255 and 453°C , and $253, 352$, and 601°C , and 268°C , respectively. The endothermic peaks were attributed to the pyrolysis of ephedrine molecules. The residual weights corresponded to metallic forms contaminated by few carbon atoms.

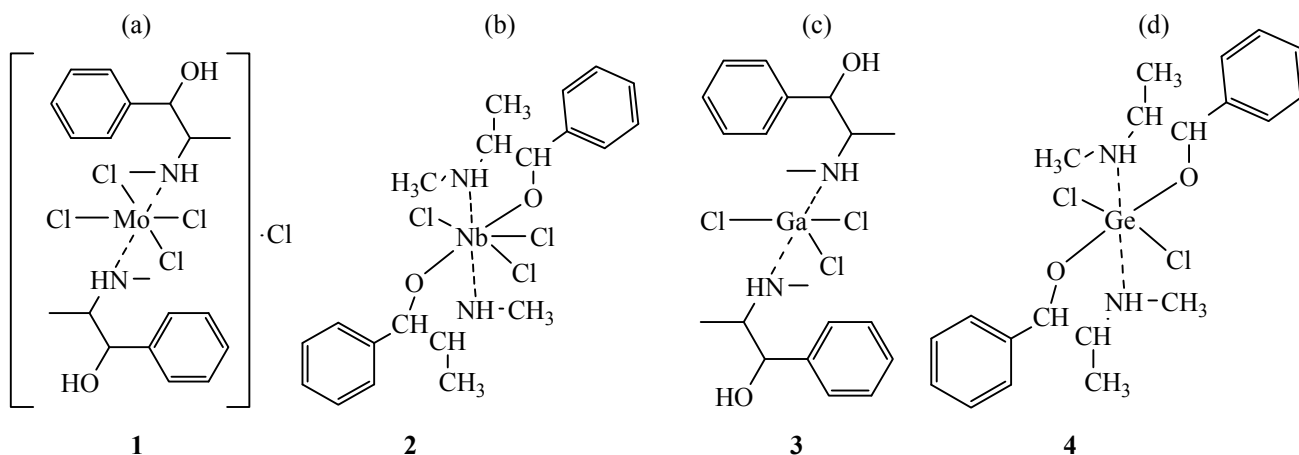


Fig. 5. Speculated structures of (a) Mo(V), (b) Nb(V), (c) Ga(III), and (d) Ge(IV) Eph complexes 1–4.

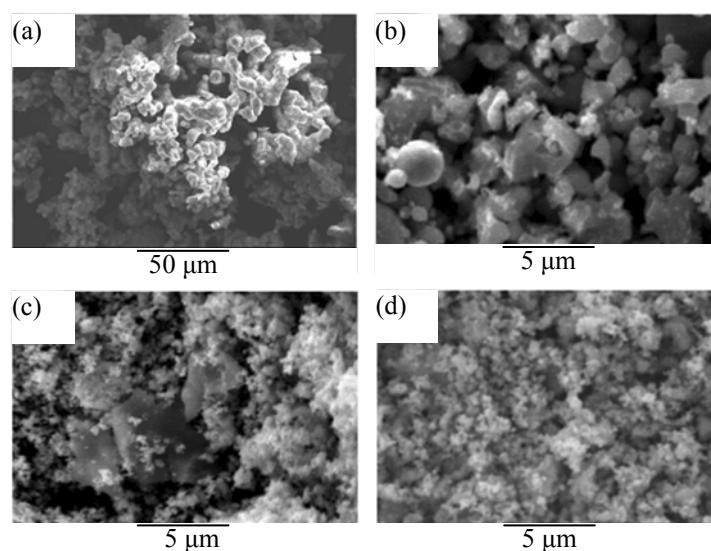


Fig. 6. SEM morphology of (a) $[\text{Mo}(\text{Eph})_2(\text{Cl})_4] \cdot \text{Cl}$, (b) $[\text{Nb}(\text{Eph})_2(\text{Cl})_3]$, (c) $[\text{Ga}(\text{Eph})_2(\text{Cl})_3]$, and (d) $[\text{Ge}(\text{Eph})_2(\text{Cl})_2]$ complexes.

Morphological studies (XRD, SEM and TEM).

X-Ray diffraction patterns of ephedrine complexes 1–4 had a crystalline to semi-crystalline nature. The characteristic diffraction pattern of the Mo(V) complex 1 included well defined peaks due to molybdenum metal at $2\theta = 32.59^\circ$, 58.22° , and 77.877° [27]. The powder XRD pattern of the Nb(V) complex 2 ($2\theta = 36.30^\circ$, 58.20° , and 68.33°) matched the standard XRD pattern of niobium metal (JCPDS card no. 035-0789) [28]. In XRD pattern of Ga(III) complex 3 significant peaks of metallic gallium [29] were observed ($2\theta = 12.44^\circ$, 13.00° , 14.40° , 15.61° , 19.10° , and 21.61°). In X-ray diffraction spectrum of Ge(IV) complex 4 the typical peaks at 29.81° , 46.93° , 57.94° , and 73.14° were recorded [30, 31]. The average of crystallite sizes of the complexes 1–4 were estimated, using the Debye–Scherrer equation [32], to be in the range of 36–71 nm.

According to SEM images (Fig. 6) the particle sizes of synthesized ephedrine complexes were within 5–50 μm . The micrographs of all complexes had a crushed snow shape with small semispherical particles. TEM micrography demonstrated that spherical particles sizes were inserted within the range of 10–50 nm.

Antimicrobial and anticancer assessments.

Antimicrobial activity of free Eph·HCl drug and its complexes 1–4 was assessed *in vitro* against bacteria [G^+ (*Escherichia coli* and *Pseudomonas aeruginosa*), G^- (*Bacillus subtilis* and *Staphylococcus aureus*), and fungi (*Aspergillus flavus* and *Candida albicans*)] (Table 2). The accumulated data demonstrated that the complexes 1–4 were more active against the bacteria and fungi than the free ligand drug due to chelation that facilitated penetration of metal ions through lipid

Table 2. Inhibition zones diameter for free Eph and its complexes 1–4 against some kinds of bacteria and fungi^a

Sample	Inhibition zone diameter, mm/mg						
	<i>Bacillus subtilis</i> (G ⁺)	<i>Escherichia coli</i> (G ⁻)	<i>Pseudomonas aeruginosa</i> (G ⁻)	<i>Staphylococcus aureus</i> (G ⁺)	<i>Aspergillus flavus</i> (Fungus)	<i>Candida albicans</i> (Fungus)	
Control: DMSO	0.0	0.0	0.0	0.0	0.0	0.0	
Tetracycline Antibacterial agent	Standard	34	32	34	30	–	–
Amphotericin B Antifungal agent		–	–	–	–	18	19
Eph–HCl		7	16	12	0.0	0.0	5
1		22	12	18	8	1	8
2	17	8	25	19	2	10	
3	24	32	12	21	5	11	
4	15	12	10	22	5	17	

^aSolvent: DMSO.**Table 3.** Inhibitory activity of Eph–Mo(V) complex 1 against HepG-2 cell lines

<i>c</i> , µg/mL	Inhibitory activity against HepG-2 cell line								SE
	absorption	<i>c</i> , %	absorption	<i>c</i> , %	absorption	<i>c</i> , %	average absorption	<i>c</i> _{average} , %	
0	0.425	100.6314	0.431	102.0521	0.411	97.3165	0.422333	100	1.40303
0.1	0.411	97.3165	0.389	92.10734	0.402	97.81022	0.400667	94.86978	1.824249
1	0.388	91.87056	0.373	88.31886	0.376	89.0292	0.379	89.73955	1.085061
10	0.385	91.16022	0.379	89.73954	0.371	87.8453	0.378333	89.5817	0.960184
100	0.386	91.397	0.356	84.29361	0.366	86.6614	0.369333	87.45068	2.088202
1000	0.236	55.88003	0.241	57.06393	0.232	54.93291	0.236333	55.95896	0.616436

Table 4. Inhibitory activity of Eph–Ga(III) complex 3 against HepG-2 cell lines

<i>c</i> , µg/mL	Inhibitory activity against HepG-2 cell line								SE
	absorption	<i>c</i> , %	absorption	<i>c</i> , %	absorption	<i>c</i> , %	average absorption	<i>c</i> _{average} , %	
0	0.425	100.6314	0.431	102.0521	0.411	97.3165	0.422333	100	1.40303
0.1	0.393	93.05446	0.375	88.88713	0.379	92.21411	0.382467	90.56039	1.27239
1	0.371	87.8453	0.387	91.63378	0.380	89.97632	0.379333	89.81848	1.096483
10	0.373	88.31886	0.363	85.95107	0.378	89.50276	0.371333	87.92424	1.044101
100	0.338	80.03157	0.346	81.92581	0.353	83.58327	0.345667	81.84689	1.026046
1000	0.215	50.90766	0.212	50.19732	0.214	50.67088	0.213667	50.59195	0.20882

membranes of cells and blocking the metal binding sites on the enzymes of the microorganism [33]. *In vitro* cytotoxicity assessments of Mo(V) and Ga(III) complexes were performed on human hepatocellular carcinoma (HepG-2) tumor cell line (Tables 3 and 4). The accumulated data for complexes **1** and **3** demonstrated IC₅₀ value to be higher than 1000 µg/mL.

CONFLICT OF INTERESTS

No conflict of interests was declared by the authors.

REFERENCES

- Schaneberg, N.T., Crockett, S., Badir, E., and Khan, I.A., *Phytochemistry*, 2003, vol. 62, p. 911. doi 10.1016/S0031-9422(02)00716-1
- Roman, M.C., *J. AOAC Int.*, 2004, vol. 87, p. 1. PMID: 15084081.
- Pellati, F., and Benvenuti, S., *J. Chromatogr. A*, 2007, vol. 1161, p. 71. doi 10.1016/j.chroma.2007.05.097
- Lieberman, R.L., Bino, A., Mirsky, N., Summers, D.A., and Thompson, R.C., *Inorg. Chim. Acta*, 2000, vol. 297, p. 1. doi 10.1016/S0020-1693(99)00251-0
- Koczoń, P., Piekut, J., Borawska, M., and Lewandowski, W., *J. Mol. Struct.*, 2003, vol. 651, p. 67. doi 10.1016/S0022-2860(02)00627-0
- Cui, X., Joannou, C.L., Hughes, M.N., and Cammack, R., *FEMS Microbiol. Lett.*, 1992, vol. 98, p. 67. doi 10.1111/j.1574-6968.1992.tb05491.
- Hueso-Urena, F., Moreno-Carretero, M., Romero-Molina, M., Salas-Peregrin, J., Sanchez-Sanchez, M., Alvarez de Cienfuegos-Lopez, G., and Faure, R., *J. Inorg. Biochem.*, 1993, vol. 51, p. 613. doi 10.1016/0162-0134(93)85033-5
- Koczoń, P., Piekut, J., Borawska, M., Świslocka, R., and Lewandowski, W., *Spectrochim Acta Part A*, 2005, vol. 61, p. 1917. doi 10.1016/j.saa.2004.07.022
- Koczoń, P., Piekut, J., Borawska, M., Świslocka, R., and Lewandowski, W., *Anal bioanal chem.*, 2006, vol. 384, p. 302. doi 10.1007/s00216-005-0158-7
- Bauer, A.W., Kirby, W.A., Sherris, C., and Turck, M., *Am. J. Clin. Pathology*, 1996, vol. 45, p. 493. PMID: 5325707.
- Pfaller, M.A., Burmeister, L., Bartlett, M.A., and Rinaldi, M.G., *J. Clin. Microbiol.*, 1988, vol. 26, p. 1437. PMID: 3049651.
- National Committee for Clinical Laboratory Standards. Performance Volume. Antimicrobial Susceptibility of Flavobacteria, 1997.
- National Committee for Clinical Laboratory Standards. Methods for Dilution Antimicrobial Susceptibility Tests for Bacteria That Grow Aerobically. Approved Standard M7-A3, Villanova, Pa, 1993.
- Mosmann, T., *J. Immunol. Methods*, 1983, vol. 65, p. 55. doi 10.1016/0022-1759(83)90303-4
- Gomha, S.M., Riyadh, S.M., Mahmmoud, E.A., and Elaasser, M.M., *Heterocycles*, 2015, vol. 91(6), p. 1227. doi 10.3987/COM-15-13210
- Refat, M.S., *J. Mol. Struct.*, 2007, vol. 842, nos. 1–3, p. 24. doi 10.1016/j.molstruc.2006.12.006
- Allinger, N.L., *J. Am. Chem. Soc.*, 1977, vol. 99, p. 8127. doi 10.1021/ja00467a001
- Hartl, F., Barbaro, P., Bell, I.M., Clark, R.J.H., Snoeck, T.L., and Vlcek, A., *Inorg. Chim. Acta*, 1996, vol. 252, p. 157. doi 10.1016/S0020-1693(96)05309-1
- Karpshin, T.B., Gehard, M.S., Solomon, E.I., and Raymond, K.N., *J. Am. Chem. Soc.*, 1991, vol. 113(8), p. 2977. doi 10.1021/ja00008a028
- Michaud-Soret, I., Andersson, K.K., and Que, L., *J. Biochem.*, 1995, vol. 34(16), p. 5504. doi 10.1021/bi00016a022
- Lewandowski, W., Kalinowska, M., and Lewandowska, H., *J. Inorg. Biochem.*, 2005, vol. 99, p. 1407. doi 10.1016/j.jinorgbio.2005.04.010
- Ohrstrom, L. and Michaud-Soret, I., *J. Phys. Chem., A*, 1999, vol. 103, p. 256. doi 10.1021/jp981508f
- Noms, A.R., Kumar, R., Buncel, E., and Beauchamp, A.L., *J. Inorg. Biochem.*, 1984, vol. 21, p. 277. doi 10.1016/0162-0134(84)85050-3
- Aldridge, S., Baker, R.J., Coombs, N.D., Jones, C., Rose, R.P., Rossin, A., and Willock, D.J., *Dalton Trans.*, 2006, p. 3313. doi 10.1039/B604640A.
- Martsinko, E.E., Seifullina, I.I., and Verbitskaya, T.G., *Russ. J. Coord. Chem.*, 2005, vol. 31(8), p. 541. doi 10.1007/s11173-005-0133-z
- Kim, H.K., Choi, Y.H., Erkelens, C., Lefeber, A.W.M., and Verpoorte, R., *Chem. Pharm. Bull.*, 2005, vol. 53, no. 1, p. 105. doi 10.1248/cpb.53.105
- Chakraborty, S.P. and Krishnamurthy, N., *J. Powder Metall. Min.*, 2013, vol. 2(3), p. 1. doi 10.4172/2168-9806.1000113
- Kumar, T.S., Kumar, S.R., Rao, M.L., and Prakash, T.L., *J. Metallurgy*, 2013, vol. 2013, p. 1, Article ID 629341. doi 10.1155/2013/629341
- Yarema, M., Wörle, M., Rossell, M.D., Erni, R., Caputo, R., Protesescu, L., Kravchyk, K.V., Dirin, D.N., Lienau, K., von Rohr, F., Schilling, A., Nachttegaal, M., and Kovalenko, M.V., *J. Am. Chem. Soc.*, 2014, vol. 136, p. 12422. doi 10.1021/ja506712d
- Gu, Z., Liu, F., Howe, J.Y., Paranthaman, M.P., and Pan, Z., *Nanoscale*, 2009, vol. 1, p. 347. doi:10.1039/B9NR00040B
- Chiu, H.W., Chervin, C.N., and Kauzlarich, S.M., *Chem. Mater.*, 2005, vol. 17, p. 4858. doi:10.1021/cm050674e
- X-Ray Diffraction Procedures for Polycrystalline and Amorphous Materials*, Klug, H.P., Ed., New York, Wiley, 1974.
- Dharmaraj, N., Viswanathamurthi, P., and Natarajan, K., *Trans. Met. Chem.*, 2001, vol. 26, p. 105. doi 10.1023/A:100713240